

# BER and Capacity/Spectral Efficiency Enhancement of MIMO Systems using Digital Antenna Arrays Beamforming

Amr H. Hussein<sup>a</sup>, Nourhan M. Salem<sup>b</sup>, Mohamed E. Nasr<sup>c</sup>, Mahmoud M. Selim<sup>d\*</sup>

<sup>a,b,c,d</sup>Department of Electronics and Electrical Communications Engineering, Faculty of Engineering, Tanta University, Tanta 31511, Egypt

<sup>a</sup>Email: [amrvips@yahoo.com](mailto:amrvips@yahoo.com), <sup>b</sup>Email: [nouraa.magdy@gmail.com](mailto:nouraa.magdy@gmail.com), <sup>c</sup>Email: [menasr2001@yahoo.com](mailto:menasr2001@yahoo.com), <sup>d</sup>Email: [mahmoud.sleem@f-eng.tanta.edu.eg](mailto:mahmoud.sleem@f-eng.tanta.edu.eg)

## Abstract

Multi-input Multi-output (MIMO) systems are of the most promising ones in the field of wireless communications as they provide high data rates and reduce the bit error rate (BER) using spatial multiplexing (SM) and diversity gain techniques, respectively. The deep review of MIMO systems shows that most of them are based on the utilization of uniform linear antennas (ULA) arrays. For further performance enhancement, a new digital array beamforming technique for linear antenna arrays optimization is introduced for both single-user and multi-user MIMO systems to achieve maximum gain. In our proposed technique, the antenna arrays are implemented for a higher gain by adjusting the feeding and the distance between the antenna elements. The modified mathematical model for our proposed digital array beamforming MIMO system has been derived and merged to the current linear detection techniques such as Maximum Likelihood (ML), Zero Forcing (ZF), and Minimum Mean Square Error (MMSE). The simulation results demonstrated the superiority of our proposed technique over the traditional MIMO systems in terms of BER and spectral efficiency (SE).

**Keywords:** MIMO; ULA array; digital beamforming; ML; ZF; BER; spectral efficiency.

---

\* Corresponding author.

## **1. Introduction**

MIMO wireless systems employ multiple transmit and receive antennas to increase the transmission data rate through spatial multiplexing or to improve system reliability in terms of bit error rate (BER) performance using space-time codes (STCs) for diversity maximization. MIMO systems exploit multipath propagation to achieve these benefits, without the expense of additional bandwidth [1]. More recent MIMO techniques such as the geometric mean decomposition (GMD) aim at combining the diversity and data rate maximization aspects of MIMO systems in an optimal manner [2]. These advantages make MIMO technology a very attractive and promising option for future mobile communication systems especially when combined with the benefits of orthogonal frequency-division multiplexing (OFDM). Many efforts attempting to improve the BER performance of MIMO systems are exerted. The research in BER enhancement can be confined in the following aspects: selecting the appropriate modulation scheme, using efficient decoding techniques, signal to noise ratio (SNR) boosting techniques, utilization of hybrid detection techniques, and utilization of analog or digital beamforming. A summary of the state-of-the-art for these techniques can be found in [3-11] and described in detail as follows. Modulation scheme can play an important role in optimizing the throughput/BER performance of MIMO and other wireless communication systems [3]. Based on the modulation scheme selection, the BER performance of MIMO-OFDM system is evaluated for various modulation schemes in [4]. The MIMO-OFDM system performance is analyzed over additive white gaussian noise (AWGN) channel using binary phase-shift keying (BPSK), quadrature phase-shift keying (QPSK), and quadrature amplitude modulation (QAM) modulation techniques. The simulation results showed that 16-QAM has better BER performance compared to BPSK and QPSK but at the expense of complexity. Also, 16-QAM provided better performance compared to 64-QAM and 256-QAM [4]. The deployment of conventional turbo codes provides higher performance in conventional MIMO systems. However, significant performance degradation occurs in the case of overloaded MIMO when the number of transmit antennas is greater than the number of receive antennas. To overcome this problem, joint turbo decoding [5] is introduced for MIMO systems. It provides significant reduction in BER at low SNR regime. However, its main drawback lies in its high computational complexity [6]. SNR is a main factor that affects the BER performance of any communication system. In this context, Maximum Likelihood (ML), Zero Forcing (ZF), and Minimum Mean Square Error (MMSE) based wavelet de-noising detectors are introduced in [7]. The received signal at each receiving antenna is firstly de-noised to boost the SNR of each branch before the application of the dedicated detector. However, utilization of de-noising filters rises up the computational complexity of the detection process. For optimum detection, the ML has the highest BER performance. However, it is time consuming and has very high complexity which increases exponentially with the number of transmit antennas and the size of constellation points. To enhance the BER performance of the low complexity Quasi-ML detectors such as Zero Forcing, and Minimum Mean Square Error, a hybrid combination between ML and low complexity Quasi-ML detectors was introduced in [8]. This technique is based on dividing the transmitted symbols vector and the channel matrix into two equal-size subsets. The Maximum Likelihood is used for the first subset in order to provide more accurate estimation of the received symbols, while the Quasi-ML detectors are used to estimate the second subset. This technique has improved the BER performance of Quasi-ML detectors, but does not exceed the performance of ML detector. On the other hand, analog beamforming, digital beamforming, and hybrid analog-digital beamforming are introduced for MIMO systems

to minimize the estimation error in the transmitted data using a fewer number of expensive radio frequency (RF) chains [9-12]. These methods achieve good performance but suffer from high complexity in the optimization of the weighted approximation gap between the optimal beamformer and the hybrid ones. In the same context, many researches attempted to synthesize large antennas arrays using a reduced number of antenna elements as introduced in [13-20]. A non-iterative algorithm based on the matrix pencil method (MPM) was introduced in [13-15]. In [19], a hybrid technique based on the combination of the method of moments (MOM) and the genetic algorithm (GA), namely MOM/GA, was introduced for arbitrarily shaped patterns synthesis using a reduced number of antenna elements. Moreover, new evolutionary algorithms based on the advanced optimization techniques are used successfully to solve the problem of complicated radiation pattern synthesis as in [20-23]. To obtain a higher gain for efficient power handling, a larger number of antennas and RF front end chains are required at the transmitting and receiving sides. In practice, low-cost and low-energy consuming RF/digital components are required to be deployed for practical MIMO systems. In this paper, a new MIMO signal model based on antenna arrays beamforming at both the transmitting and receiving sides is introduced for BER and capacity/SE enhancement. This proposed beamforming method improves the SNR of the received MIMO signal via increasing the transmitting and receiving antenna gains. For a fixed number of data streams or for a given  $N_T \times N_R$  MIMO system, where  $N_T$  and  $N_R$  are the number of antenna elements at the transmitter and receiver, respectively, the existing antenna arrays are beamformed to synthesize an antenna array with a larger size to provide higher gains without using additional antenna elements. Several beamforming and simulation scenarios are performed to verify the effectiveness of the proposed beamforming-based signal model on the performance of the traditional MIMO detection techniques such as Maximum Likelihood (ML) and Zero Forcing (ZF). The remaining part of this paper is organized as follows. The problem is mathematically formulated in Section 2. Our proposed beamforming-based MIMO signal model is introduced in Section 3. The merge of our proposed method into traditional MIMO detection techniques is introduced in Section 4. The capacity of the proposed beamforming scheme is analyzed in Section 5. Simulation setup, results and discussion are provided in Section 6. The paper is finally concluded in Section 7.

## 2. Problem formulation

Consider the traditional  $N_T \times N_R$  MIMO system model shown in Figure 1, where  $N_T$  and  $N_R$  are the number of transmitting and receiving antennas, respectively. The antenna elements are uniformly fed and linearly aligned with uniform spacing  $d = \lambda/2$ , where  $\lambda$  is the corresponding wavelength, constructing a uniform linear antenna array (ULA). The received signal  $y$  is given by [24]:

$$y = \sqrt{\frac{E_x}{N_T}} \mathbf{H}x + \mathbf{v}, \quad (1)$$

where  $x \in \mathbb{C}^{N_T \times 1}$  is the baseband signal vector transmitted during each symbol period formed by the antenna elements and  $E_x$  is the power of the transmitted signal. It is assumed that the average power constraint across all transmit antennas is equal to  $E_x$ , such that  $E[xx^H] = E[|x|^2] \leq E_x$ . In this case,  $E_x/N_T$  is the input power assigned for each antenna.  $y \in \mathbb{C}^{N_R \times 1}$  denotes the received symbol vector where  $N_T \leq N_R$ .  $\mathbf{v} \in \mathbb{C}^{N_R \times 1}$  is a zero-mean circular symmetric complex Gaussian (ZMCSCG) noise vector with variance  $\sigma^2$ .  $\mathbf{H} \in \mathbb{C}^{N_R \times N_T}$  is the

channel matrix which represents the scattering effects of the channel. For simplicity, the channel matrix  $\mathbf{H}$  is considered to be known at the receiver. In traditional MIMO systems, the utilization of limited gain ULAs at the transmitting and receiving sides largely affects the SNR performance. In order to enhance the SNR by increasing the antenna arrays gains, each array size should be increased. Consequently, the number of RF chains, number of data streams, system complexity, and cost are increased. For this purpose, the beamforming is considered as the key solution for these problems.

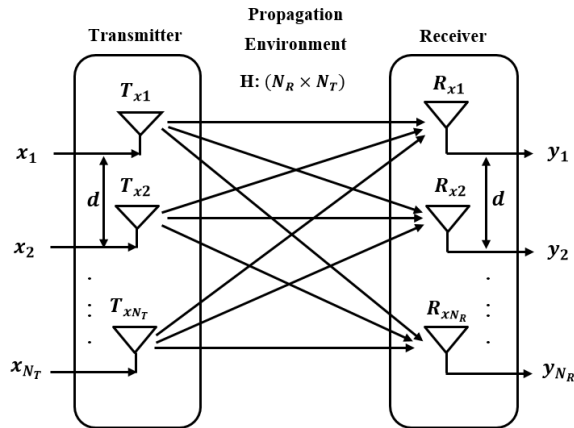
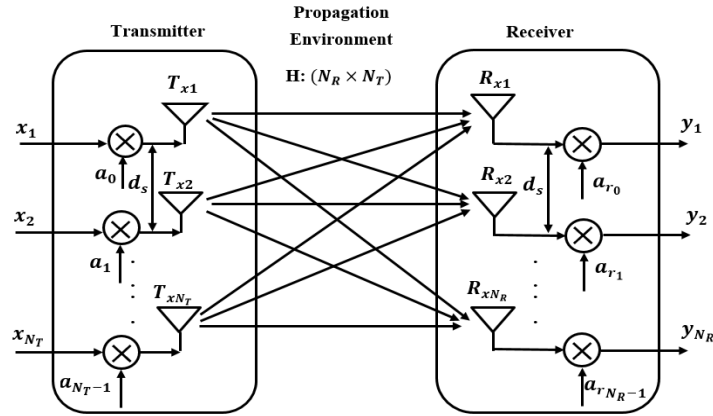


Figure 1: Traditional MIMO system model with  $N_T$  transmit antennas and  $N_R$  receive antennas

### 3. Proposed beamforming-based MIMO signal model

In this section, the proposed beamforming-based MIMO signal model is derived. It is well known that the traditional MIMO system employs limited gain ULAs at both the transmitting and receiving sides. However, in order to obtain higher antenna arrays gains for efficient power handling, a larger number of antennas is required. This problem can be avoided using antenna arrays beamforming. One of the most promising aspects of beamforming is the antenna arrays synthesis using a reduced number of antenna elements. The synthesized arrays almost have the same radiation characteristics of the arrays with a larger size such as; array gain, half power beamwidth (HPBW), and side lobe level (SLL). However, in this case, the reverse beamforming process is executed, where, a fewer number of antenna elements are used to synthesize various larger size antenna arrays by controlling the elements excitations and spacing. The number of antenna elements of the large-size arrays is constrained by the appearance of grating lobes in the synthesized pattern. Consequently, higher antenna gains are achieved without using additional antenna elements. As the synthesized excitation coefficients are no longer uniform, the beamforming-based MIMO system model can be drawn as shown in Figure 2.



**Figure 2:** Proposed  $N_T \times N_R$  MIMO model applying beamforming at both transmitting and receiving sides

Beamforming will boost the SNR of the received signal proportional to the gain increments of the synthesized arrays at each side. Therefore, the MoM/GA array synthesis technique introduced in [17] is used to synthesize the radiation pattern of a desired large size antenna array using a fewer number of antenna elements as shown in Figure 2. The MoM/GA is a hybrid combination between the Method of Moments (MoM) and the Genetic Algorithm (GA). It combines the benefits of both the numerical and optimization solutions represented in MoM and GA, respectively. For a given number of antenna elements, the MoM/GA determines the elements excitations and spacing required to synthesize the desired pattern either a pencil beam or a shaped beam pattern. Applying beamforming at the transmitting side, the synthesized array factor  $AF_{st}(\theta)$  should be coincided with the desired large size array factor  $AF_t(\theta)$  which can be expressed as follows:

$$AF_{st}(\theta) \approx AF_t(\theta)$$

$$\sum_{p=0}^{N_T-1} a_p e^{jk p d_{st} \cos(\theta)} \approx \sum_{m=0}^{M_T-1} a_m e^{jk m d \cos(\theta)}, \quad (2)$$

where  $M_T$  is the number of elements of the desired large size array and  $N_T$  is the number of elements of the synthesized array where  $M_T > N_T$ .  $a_m$  and  $a_p$  are the excitation coefficients of the desired and synthesized arrays, respectively.  $d$  and  $d_{st}$  are the element spacings of the desired and synthesized arrays, respectively. At the receiving side, the array factor of the desired large size array  $AF_r(\theta)$  and the synthesized array factor  $AF_{sr}(\theta)$  should be also coincided as follows:

$$AF_{sr}(\theta) \approx AF_r(\theta)$$

$$\sum_{l=0}^{N_R-1} a_{rl} e^{jk l d_{sr} \cos(\theta)} \approx \sum_{r=0}^{M_R-1} a_r e^{jk r d \cos(\theta)}, \quad (3)$$

where  $M_R$  is the number of elements of the desired large size array and  $N_R$  is the number of elements of the synthesized array such that  $M_R > N_R$ .  $a_r$  and  $a_{rl}$  are the excitation coefficients of the desired and synthesized

arrays, respectively and  $d_{sr}$  is the element spacing of the synthesized array. The MoM/GA solves Eq. (2) and Eq. (3) to determine the synthesized array parameters ( $a_p, a_{r1}, d_{st}$ , and  $d_{sr}$ ) to construct the beamformed MIMO system shown in Figure 2. Based on Eq. (1), the beamforming-based MIMO signal model can be derived as follows:

**Step 1:** Applying beamforming at the transmitting side only, the received signal at the receiving antenna array without beamforming,  $y_r$ , can be written as follows:

$$y_r = \sqrt{\frac{E_x}{N_T}} \mathbf{H} (A_t \cdot x) + v, \tag{4}$$

where  $(\cdot)$  is the element-by-element multiplication and  $A_t$  is the transmitting steering vector.

**Step 2:** If the beamforming is applied at both the transmitting and receiving sides, the overall beamforming based received signal  $y_{BF}$  will be the element-by-element multiplication of the received signal  $y_r$  and the receiving steering vector  $A_r$  which can be expressed as:

$$y_{BF} = \sqrt{\frac{E_x}{N_T}} (\mathbf{H} (A_t \cdot x) + v) \cdot A_r, \tag{5}$$

or

$$y_{BF} = \sqrt{\frac{E_x}{N_T}} (\mathbf{H} (A_t \cdot x)) \cdot A_r + v \cdot A_r, \tag{6}$$

where  $y_{BF}$  is the received signal using beamformed/synthesized antenna arrays at both the transmitting and receiving sides.  $A_t$  is the transmitting steering vector which is derived from the synthesized array factor  $AF_{st}(\theta)$  substituting  $\theta = \theta_i$ .  $A_r$  is the receiving steering vector which is derived from the synthesized array factor  $AF_{sr}(\theta)$  substituting  $\theta = \theta_i$ . Consider the case that the transmitting and receiving antenna arrays are aligned together in the broadside direction, where the main beam direction is at  $\theta_i = 90^\circ$  with respect to the array line. The steering vectors at the broadside direction can be written as follows:

$$A_t = AF_{st}(90^\circ), \tag{7}$$

$$A_t = [a_0 \ a_1 \ a_2 \ \dots \ \dots \ \dots \ a_{N_T-1}]^T, \tag{8}$$

$$A_r = AF_{sr}(90^\circ), \tag{9}$$

$$A_r = [a_{r0} \ a_{r1} \ a_{r2} \ \dots \ \dots \ \dots \ a_{r_{N_R-1}}]^T, \tag{10}$$

$$x = [x_1(n) \ x_2(n) \ x_3(n) \ \dots \ \dots \ \dots \ x_{N_T}(n)]^T, \tag{11}$$

$$x_n(n) = [x_n(1) \ x_n(2) \ x_n(3) \ \dots \ x_n(N)]^T, \quad (12)$$

$$v = [v_1(n) \ v_2(n) \ v_3(n) \ \dots \ v_{N_T}(n)]^T, \quad (13)$$

$$v_n(n) = [v_n(1) \ v_n(2) \ v_n(3) \ \dots \ v_n(N)]^T, \quad (14)$$

$$y_{BF} = [y_1(n) \ y_2(n) \ y_3(n) \ \dots \ y_{N_R}(n)]^T, \quad (15)$$

$$y_n(n) = [y_n(1) \ y_n(2) \ y_n(3) \ \dots \ y_n(N)]^T, \quad (16)$$

where  $N$  is the number of samples of the received signal and  $[ ]^T$  is the matrix transpose. For simplicity, Eq. (5) can be expressed in matrix form as follows:

$$y_{BF} = \sqrt{\frac{E_x}{N_T}} \begin{bmatrix} h_{11} & h_{12} & \dots & h_{1N_T} \\ h_{21} & h_{22} & \dots & h_{2N_T} \\ \dots & \dots & \dots & \dots \\ h_{N_R1} & h_{N_R2} & \dots & h_{N_RN_T} \end{bmatrix} \begin{bmatrix} a_0 \\ a_1 \\ \dots \\ a_{N_T-1} \end{bmatrix} \begin{bmatrix} x_1(n) \\ x_2(n) \\ \dots \\ x_{N_T}(n) \end{bmatrix} + \begin{bmatrix} v_1(n) \\ v_2(n) \\ \dots \\ v_{N_R}(n) \end{bmatrix} \begin{bmatrix} a_{r_0} \\ a_{r_1} \\ \dots \\ a_{r_{N_R-1}} \end{bmatrix}. \quad (17)$$

Then,

$$y_{BF} = \sqrt{\frac{E_x}{N_T}} \times \begin{bmatrix} h_{11} & h_{12} & \dots & h_{1N_T} \\ h_{21} & h_{22} & \dots & h_{2N_T} \\ \dots & \dots & \dots & \dots \\ h_{N_R1} & h_{N_R2} & \dots & h_{N_RN_T} \end{bmatrix} \begin{bmatrix} a_0 \\ a_1 \\ \dots \\ a_{N_T-1} \end{bmatrix} \begin{bmatrix} x_1(n) \\ x_2(n) \\ \dots \\ x_{N_T}(n) \end{bmatrix} + \begin{bmatrix} a_{r_0} \\ a_{r_1} \\ \dots \\ a_{r_{N_R-1}} \end{bmatrix} \begin{bmatrix} v_1(n) \\ v_2(n) \\ \dots \\ v_{N_R}(n) \end{bmatrix} \begin{bmatrix} a_{r_0} \\ a_{r_1} \\ \dots \\ a_{r_{N_R-1}} \end{bmatrix}. \quad (18)$$

Let  $C = \text{diag}(A_r)$  which is an  $N_R \times N_R$  matrix whose diagonal is the receiving steering vector such that

$$C = \begin{bmatrix} a_{r_0} & 0 & \dots & 0 \\ 0 & a_{r_1} & \dots & 0 \\ \dots & \dots & \dots & \dots \\ 0 & 0 & \dots & a_{r_{N_R-1}} \end{bmatrix}. \quad (19)$$

Let  $W = \text{diag}(A_t)$  which is an  $N_T \times N_T$  matrix whose diagonal is the transmitting steering vector which can be written as follows:

$$W = \begin{bmatrix} a_0 & 0 & \dots & 0 \\ 0 & a_1 & \dots & 0 \\ \dots & \dots & \dots & \dots \\ 0 & 0 & \dots & a_{N_T-1} \end{bmatrix}. \quad (20)$$

Substituting Eq. (19) and Eq. (20) in Eq. (18), it can be rewritten as follows:

$$y_{BF} = \sqrt{\frac{E_x}{N_T}} C H W x + C v. \quad (21)$$

Let  $\mathcal{H} = \mathbf{C}\mathbf{H}\mathbf{W}$ , and  $\boldsymbol{\omega} = \mathbf{C}\mathbf{v}$  is the  $N_R \times 1$  weighted noise vector. Then, the general form of the proposed beamforming-based MIMO signal model is given by:

$$y_{BF} = \sqrt{\frac{E_x}{N_T}} \mathcal{H}x + \boldsymbol{\omega} \quad (22)$$

#### 4. Application of the proposed signal model to MIMO detection algorithms

In this section, two beamforming-based MIMO detection algorithms are introduced, where, the proposed signal model expressed in Eq. (22) is applied for both Maximum Likelihood (ML) and Zero Forcing (ZF) detectors. The detection algorithms are denoted as ML with beamforming (MLWBF) and ZF with beamforming (ZFWBF).

##### 4.1. Beamforming-based ML detector (MLWBF)

Considering the received signal model given in Eq. (1), the ML detection problem consists of determining the transmitted vector  $\hat{x}$  with the highest posteriori probability or based on the minimum Euclidean distance. The squared Euclidean distance of all possible symbols with the received vector in the signal space diagram is calculated and then the minimum of all those combinations is selected. This is typically carried out in practice by means of solving the following least squares problem:

$$\hat{x} = \mathop{\text{arg min}}_{x \in X^N} \left\| y - \sqrt{\frac{E_x}{N_T}} \mathbf{H}x \right\|^2 \quad (23),$$

where  $\| \cdot \|$  denotes the 2-norm and  $\hat{x}$  is an  $2N_T$  dimensional vector whose entries belong to an M-ary alphabet. Eq. (23) is often called the ML detection rule [8]. Using the proposed signal model expressed in Eq. (22), the ML expression can be rewritten as follows:

$$\hat{x} = \mathop{\text{arg min}}_{x \in X^N} \left\| y_{BF} - \sqrt{\frac{E_x}{N_T}} \mathcal{H}x \right\|^2 \quad (24).$$

##### 4.2. Beamforming-based ZF detector (ZFWBF)

According to Eq. (1), the traditional ZF detection is a low complexity linear detection algorithm that gives the estimate of  $x$  as given in [8].

$$\hat{x} = \mathbf{H}^\dagger y = \sqrt{\frac{E_x}{N_T}} x + (\mathbf{H}^H \mathbf{H})^{-1} \mathbf{H}^H v = \sqrt{\frac{E_x}{N_T}} x + \hat{v}_{zf}. \quad (25)$$

The detector thus forces the interference to zero. The matrix  $\mathbf{H}^\dagger$  nullifying the interference is given by:

$$\mathbf{H}^\dagger = (\mathbf{H}^H \mathbf{H})^{-1} \mathbf{H}^H, \quad (26)$$

where  $\mathbf{H}^\dagger$  is the pseudo inverse of the channel matrix  $\mathbf{H}$ . Using the proposed signal model expressed in Eq. (22), the ZF detection process applying beamforming can be summarized as follows:

1. Calculate the transmitting and receiving steering vectors  $A_t$  and  $A_r$ .
2. Construct both  $\mathbf{W} = \text{diag}(A_t)$  and  $\mathbf{C} = \text{diag}(A_r)$  matrices.
3. Construct the matrix  $\mathcal{H} = \mathbf{C}\mathbf{H}\mathbf{W}$ .
4. Determine the pseudo inverse of the new matrix  $\mathcal{H}$  which is given by  $\mathcal{H}^\dagger = (\mathcal{H}^H\mathcal{H})^{-1}\mathcal{H}^H$ .
5. The estimates of  $x$  are determined as  $\hat{x} = \mathcal{H}^\dagger y_{BF}$ .

### 5. Capacity of the proposed beamforming-based MIMO system

The capacity of the traditional  $N_T \times N_R$  MIMO system can be expressed as introduced in [24].

$$C = \max_{\text{Tr}(\mathbf{R}_{xx})=N_T} \log_2 \det \left( \mathbf{I}_{N_R} + \frac{E_x}{N_o N_T} \mathbf{H} \mathbf{R}_{xx} \mathbf{H}^H \right) \text{ bps/Hz} \quad (27),$$

where  $N_o$  is the power spectral density of the ZMCSCG noise.  $\mathbf{I}_{N_R}$  is the identity matrix where  $\mathbf{I}_{N_R} \in \mathbb{C}^{N_R \times N_R}$ . The noise covariance matrix  $\mathbf{R}_{vv} = E\{vv^H\} = N_o \mathbf{I}_{N_R}$ .  $\mathbf{R}_{xx}$  is the covariance matrix of the transmitted signal vector  $x$  where  $\mathbf{R}_{xx} = E\{xx^H\}$ . To derive an expression for the capacity of the proposed system, we determine the covariance matrix  $\mathbf{R}_{yy}$  of the proposed beamforming-based MIMO signal model of Eq. (22) as follows.

$$\begin{aligned} \mathbf{R}_{yy} &= E\{y_{BF} y_{BF}^H\}, \\ &= E \left\{ \left( \sqrt{\frac{E_x}{N_T}} \mathcal{H} x + \omega \right) \left( \sqrt{\frac{E_x}{N_T}} x^H \mathcal{H}^H + \omega^H \right) \right\}, \\ &= \frac{E_x}{N_T} E\{(\mathcal{H} x x^H \mathcal{H}^H + \omega \omega^H)\}, \\ &= \frac{E_x}{N_T} \mathcal{H} E\{x x^H\} \mathcal{H}^H + E\{\omega \omega^H\}, \\ &= \frac{E_x}{N_T} \mathbf{C} \mathbf{H} \mathbf{W} E\{x x^H\} \mathbf{W}^H \mathbf{H}^H \mathbf{C}^H + \mathbf{C} E\{v v^H\} \mathbf{C}^H, \\ &= \frac{E_x}{N_T} \mathbf{C} \mathbf{H} \mathbf{W} \mathbf{R}_{xx} \mathbf{W}^H \mathbf{H}^H \mathbf{C}^H + \mathbf{C} \mathbf{R}_{vv} \mathbf{C}^H, \\ &= \frac{E_x}{N_T} \mathbf{C} \mathbf{H} \mathbf{W} \mathbf{R}_{xx} \mathbf{W}^H \mathbf{H}^H \mathbf{C}^H + \mathbf{C} N_o \mathbf{I}_{N_R} \mathbf{C}^H. \end{aligned} \quad (28)$$

Based on Shannon capacity rule introduced in [24], the achievable capacity  $C_{BF}$  will be expressed in (bps/Hz) as:

$$C_{BF} = \max_{\text{Tr}(\mathbf{R}_{xx})=N_T} \log_2 \det \left( \mathbf{I}_{N_R} + \frac{E_x}{N_o N_T} (\mathbf{C} \mathbf{I}_{N_R} \mathbf{C}^H)^{-1} \mathbf{C} \mathbf{H} \mathbf{W} \mathbf{R}_{xx} \mathbf{W}^H \mathbf{H}^H \mathbf{C}^H \right) \quad (29).$$

The percentage capacity enhancement ratio can be calculated as

$$\tilde{\eta} = \left( \frac{C_{BF}-C}{C} \times 100 \right) \% \tag{30}$$

### 6. Simulation results and discussions

In this section, many numerical simulations are carried out to analyze the impact of the proposed digital beamforming-based signal model on the BER performance and capacity/SE of the MIMO systems. In the simulations, the standard  $4 \times 4$ ,  $8 \times 8$  LTE MIMO, and  $4 \times 12$  MIMO systems are taken as the simulation objects. The parameters specifications of the standard MIMO systems used in simulations are listed in Table 1. Based on these parameters, three beamforming scenarios are introduced to synthesize ( $N_T = N_R = 4$  elements), ( $N_T = N_R = 8$  elements), and ( $N_T = 4, N_R = 12$  elements) antenna arrays for maximum gains.

**Table 1:** Simulation parameters of the standard LTE MIMO systems

Parameters	Specifications
$N_T$	4 or 8
$N_R$	4 or 8
Antenna array type	ULA
Antenna element spacing $d$	$\lambda/2$
Number of samples $N$	1000
Channel	Rayleigh fading
Noise	ZMCSCG
Modulation technique	4-QAM

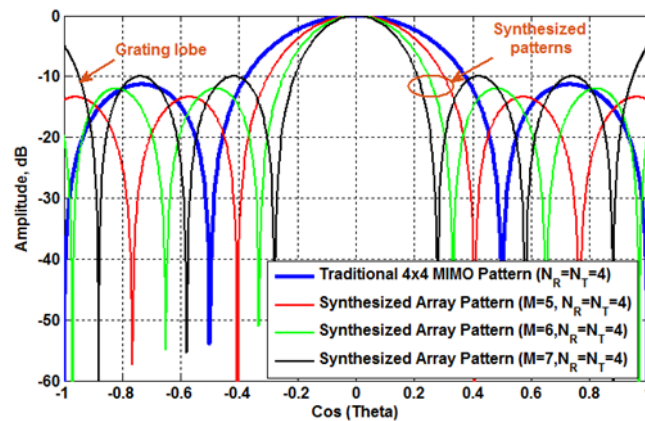


**Figure 3:** Comparison between the radiation pattern of the traditional  $4 \times 4$  LTE MIMO and the synthesized arrays patterns for  $M=5,6$  and  $7$  antenna elements.

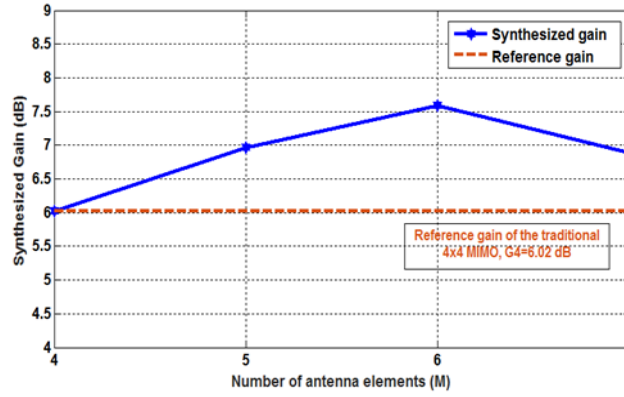


**Figure 4:** The synthesized array gain versus number of antenna elements  $M$  compared to the ordinary  $N_T=N_R=4$  array gain in case of  $4 \times 4$  LTE MIMO

**6.1. Scenario (1): Beamforming for  $4 \times 4$  LTE MIMO system**

Applying the MOM/GA array synthesis technique introduced in [19], the existing ( $N_T = N_R = 4$  elements) are used to synthesize several desired larger size antenna arrays consisting of  $M_T = M_R = M = 5, 6,$  and  $7$  elements. Figure 3 shows a comparison between the radiation pattern of the traditional  $4 \times 4$  LTE MIMO array and the synthesized arrays patterns for  $M = 5, 6,$  and  $7$  elements. The synthesized arrays patterns using  $N_T = N_R = 4$  elements are highly coincided with the ordinary  $M = 5$  and  $M = 6$  elements ULAs patterns. They have approximately the same half power beamwidth, directivity, and gain. But, as the number of elements increase above  $M = 6$ , the side lobe level increases and the grating lobes appear in the synthesized pattern as in case of  $M = 7$ . The synthesized array gain,  $G_{sM}$ , versus number of antenna elements,  $M$ , is shown in Figure 4. The synthesized array gains for  $M = 5, 6,$  and  $7$  elements calculated by the numerical integration of the array factors are  $G_{s5} = 6.9 \text{ dB}$ ,  $G_{s6} = 7.5 \text{ dB}$ , and  $G_{s7} = 6.8 \text{ dB}$ , respectively. While the array gains of the ordinary broadside ULAs,  $G_M$ , for  $M = 4, 5, 6,$  and  $7$  elements are  $G_4 = 6.0 \text{ dB}$ ,  $G_5 = 6.9 \text{ dB}$ ,  $G_6 = 7.7 \text{ dB}$ , and  $G_7 = 8.4 \text{ dB}$ , respectively, which are calculated by Eq. (31) as introduced in [25]. It is clear that, the synthesized array for  $M = 6$  elements provide the maximum gain which can be expressed as

$$G_M = 10 \log\left(\frac{2Md}{\lambda}\right). \tag{31}$$

The gain increment which is defined as the difference between the synthesized large size array gain and the ordinary array gain can be written as follows:

$$\Delta G = G_{sM} - G_{N_T}, \tag{32}$$

where  $G_{N_T} = 10 \log\left(\frac{2N_T d}{\lambda}\right)$  is the array gain of ordinary array consisting of  $N_T$  antenna elements. The ordinary arrays parameters such as half power beamwidth ( $HPBW$ ), side lobe level ( $SLL$ ), and gain  $G_M$  compared to the synthesized arrays parameters such as synthesized ( $HPBW_s$ ), synthesized ( $SLL_s$ ), synthesized gain ( $G_{sM}$ ), and gain increments  $\Delta G$  ( $dB$ ) are listed in Table 2. It is clear that, as the number of antenna elements of the large

size array to be synthesized increases, the gain increment increases. The maximum achievable gain increment occurs at  $M = 6$ . But, as the number of elements increases above  $M = 6$ , the gain increment decreases due to the appearance of grating lobes. This increase in the synthesized arrays gains at transmitting and receiving sides will boost the received signal to noise ratio of the traditional MIMO system ( $SNR_r$ ) by the value of array gain increment  $\Delta G$ . Hence, for  $N_T = N_R$ , the signal to noise ratio of the beamformed MIMO system  $SNR_{BF}$  can be calculated by:

$$SNR_{BF} = (SNR_r + \Delta G)dB. \tag{33}$$

That is because the signal power is increased in proportional to the gain increments of both synthesized antenna arrays at transmitting and receiving sides. While, the noise power is enhanced only by the gain increment of the synthesized array at receiving side as given in Eq. (21). From this point of view, the significant effect of the beamforming appears in increasing the signal to noise ratio of the MIMO system which consequently improves its BER performance and capacity without the need for array size extension or utilization of de-noising techniques.

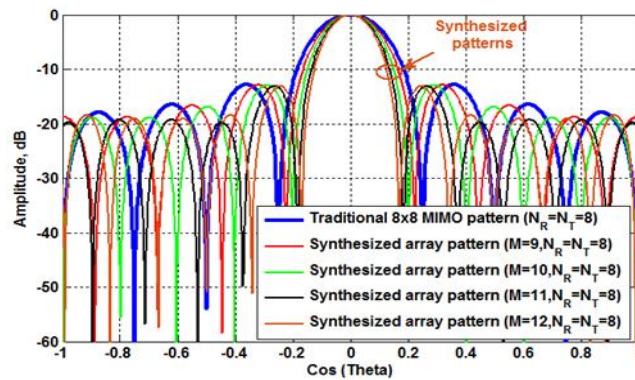


**Figure 5:** Comparison between the radiation pattern of the traditional 8×8 LTE MIMO and the synthesized arrays patterns for M=9,10,11,and 12 antenna elements

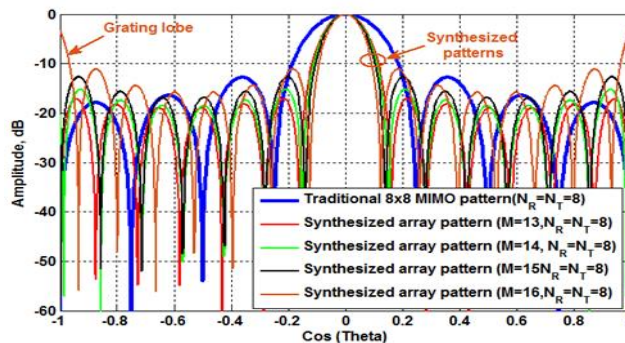


**Figure 6:** Comparison between the radiation pattern of the traditional 8×8 LTE MIMO and the synthesized arrays patterns for M=13,14,15,and 16 antenna elements

**6.2. Scenario (2): Beamforming for 8 × 8 LTE MIMO system**

Based on the previous discussion, a more complicated situation to verify the effectiveness of the proposed algorithm is taken into account. Consider the aforementioned  $8 \times 8$  MIMO system whose parameters are listed in Table 1.

**Table 2:** The parameters of the synthesized antenna arrays using  $N_T=N_R=4$  elements for  $M=5,6,$ and 7 elements antenna arrays compared to the parameters of ordinary antenna arrays

Synthesized arrays parameters using MoM/GA [19] for $N_T = N_R = 4$ elements and $G_4 = 6.0$ dB			
$M$	5	6	7
$d_s$	$0.653\lambda$	$0.768\lambda$	$0.862\lambda$
$a_1$	1.1349	1.3933	1.2988
$a_2$	1.3479	1.4797	1.1385
$a_3$	1.3479	1.4797	1.1385
$a_4$	1.1349	1.3933	1.2988
HPBW (degrees)	$20.7^\circ$	$17.1^\circ$	$14.58^\circ$
HPBW <sub>s</sub> (degrees)	$20.7^\circ$	$17.1^\circ$	$14.58^\circ$
SLL (dB)	-12.0	-12.4	-12.7
SLL <sub>s</sub> (dB)	-13.4	-12.0	-4.9
$G_M$ (dB)	7.0	7.8	8.5
$G_{sM}$ (dB)	7.0	7.6	6.9
$\Delta G = G_{sM} - G_4$ (dB)	0.9	1.6	0.9

**Table 3:** The parameters of the synthesized antenna arrays using  $N_T=N_R=8$  elements for  $M=9$  to  $M=12$  elements antenna arrays

Synthesized array parameters using MoM/GA [19] for $N_T = N_R = 8$ elements and $G_8 = 9.0$ dB				
$M$	9	10	11	12
$d_s$	$0.564\lambda$	$0.626\lambda$	$0.701\lambda$	$0.75\lambda$
$a_1$	1.089	1.1930	1.2061	1.3415
	2			
$a_2$	1.144	1.2673	1.3920	1.4908
$a_3$	1.119	1.2494	1.4952	1.5509
	6			
$a_4$	1.130	1.2518	1.3518	1.479
	7			
$a_5$	1.130	1.2518	1.3518	1.479
	7			
$a_6$	1.119	1.2494	1.4952	1.5509
	6			
$a_7$	1.144	1.2673	1.3920	1.4908
$a_8$	1.089	1.1930	1.2061	1.3415
	2			
$G_M$ (dB)	9.5	10	10.4	10.8
$G_{sM}$ (dB)	9.5	10	10.4	10.7
$\Delta G = (G_{sM} - G_8)$	0.5	0.9	1.3	1.7

Applying the array synthesis algorithm presented in [19], the dedicated  $N_T = N_R = 8$  elements are used to synthesize different larger size antenna arrays from  $M = 9$  to  $M = 16$  as shown in Figure 5 and Figure 6. The

synthesized array gain,  $G_{SM}$ , versus number of antenna elements,  $M$ , is plotted in Figure 7. It is clear that as  $M$  increases, the synthesized array gain increases until  $M = 14$  elements. For  $M \geq 15$ , the grating lobes appear significantly and the synthesized gain decreases. The synthesized array parameters, excitation coefficients, and gain increments are listed in Table 3 and Table 4.

**Table 4:** The parameters of the synthesized antenna arrays using  $N_T=N_R=8$  elements for  $M=13$  to  $M=16$  elements antenna arrays

Synthesized array parameters using MoM/GA [19] for $N_T = N_R = 8$ elements and $G_8 = 9.0$ dB				
$M$	9	10	11	12
$d_s$	$0.564\lambda$	$0.626\lambda$	$0.701\lambda$	$0.75\lambda$
$a_1$	1.089	1.1930	1.2061	1.3415
	2			
$a_2$	1.144	1.2673	1.3920	1.4908
$a_3$	1.119	1.2494	1.4952	1.5509
	6			
$a_4$	1.130	1.2518	1.3518	1.479
	7			
$a_5$	1.130	1.2518	1.3518	1.479
	7			
$a_6$	1.119	1.2494	1.4952	1.5509
	6			
$a_7$	1.144	1.2673	1.3920	1.4908
$a_8$	1.089	1.1930	1.2061	1.3415
	2			
$G_M$ (dB)	9.5	10	10.4	10.8
$G_{SM}$ (dB)	9.5	10	10.4	10.7
$\Delta G = (G_{SM} - G_8)$	0.5	0.9	1.3	1.7

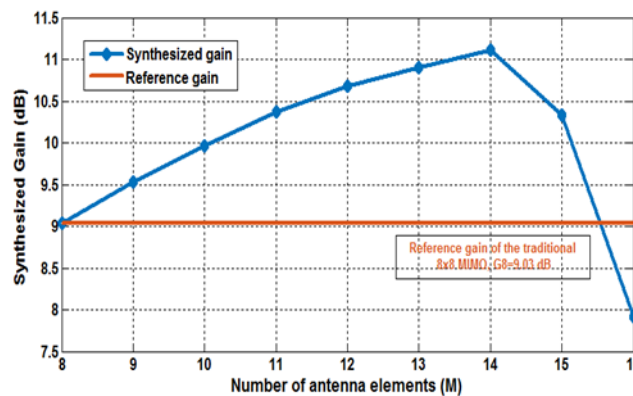


**Figure 7:** The synthesized array gain versus number of antenna elements  $M$  compared to the ordinary  $N_T=N_R=8$  array gain in case of  $8 \times 8$  LTE MIMO

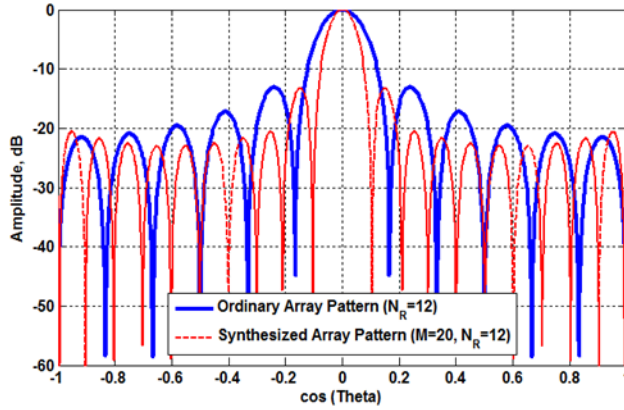


**Figure 8:** Synthesized array pattern using 12 elements for large array size consisting of  $M_R=20$  elements compared to the ordinary  $N_R=12$  elements array pattern

**6.3. Scenario (3): Beamforming for  $4 \times 12$  MIMO system**

Overloaded MIMO refers to MIMO system having  $N_R > N_T$ . In this case, the  $4 \times 12$  MIMO is taken as a simulation target. Form scenario (1), the  $N_T = 4$  elements can be used to synthesize large antenna array of size  $M_t = 6$  elements for maximum gain which equals **7.6 dB**. While for  $N_R = 12$  elements, the maximum synthesized array gain is achieved at  $M_R = 20$  elements as shown in Figure 8. For  $M_R > 20$ , the grating lobes appear in the synthesized pattern. The synthesized array gain for  $M_R = 20$  elements using only 12 elements equals **25.7 dB** which is **4.1 dB** greater than the gain of the traditional  $N_R = 12$  elements array which equals **21.6 dB**. The synthesized excitations for  $M_R = 20, N_R = 12$  elements are listed in Table 5.

**Table 5:** Synthesized array parameters using  $N_R=12$  elements for  $M_R=20$  elements large size array

Synthesized array parameters using MoM/GA [19] for $M_R = 20, N_R = 12,$ and $d_{sr} = 0.83\lambda$	
$a_{r0}$	1.383
$a_{r1}$	1.528
$a_{r2}$	1.716
$a_{r3}$	1.762
$a_{r4}$	1.683
$a_{r5}$	1.593
$a_{r6}$	1.593
$a_{r7}$	1.683
$a_{r8}$	1.762
$a_{r9}$	1.716
$a_{r10}$	1.528
$a_{r11}$	1.383

**6.4. Test case 1: ML detector using beamforming for 4 × 4 LTE MIMO system**

Considering the LTE MIMO system whose parameters are listed in Table 1, the BER performances of the traditional ML detector and the beamforming-based ML detector are analyzed. Based on the beamforming results introduced in scenario (1) for 4 × 4 LTE MIMO, the BERs versus the SNR for MLWBF compared to the traditional ML detector are plotted as shown in Figure 9. The simulation results revealed that as the number of antenna elements increases from  $M = 5$  to  $6$ , the BER performance is improved. For example, at  $SNR = 0$  dB, the estimated BER is reduced from  $1.26 \times 10^{-1}$  for conventional ML to  $5.2 \times 10^{-2}$  and  $2.4 \times 10^{-2}$  for MLWBF using  $M = 5$  and  $M = 6$  elements, respectively. On the other hand, as the number of elements increases above  $M = 6$ , i.e.  $M = 7$ , the BER is highly degraded due to the appearance of grating lobes and the increase in side lobe level as previously declared in scenario (1).

**6.5. Test case 2: ZF detector using beamforming for 4 × 4 LTE MIMO system**

In this case, the BERs versus SNR for ZFWBF compared to the traditional ZF detector are plotted as shown in Figure 10. The simulation results revealed that as the number of antenna elements increases from  $M = 5$  to  $M = 6$ , the BER is reduced. At  $SNR = 0$  dB, the estimated BER is reduced from  $5.84 \times 10^{-1}$  for conventional ZF to  $4.64 \times 10^{-1}$  and  $3.83 \times 10^{-1}$  for ZFWBF using  $M = 5$  and  $M = 6$  elements, respectively. However, as the number of elements increases above  $M = 6$ , i.e.,  $M = 7$ , the BER is highly degraded.

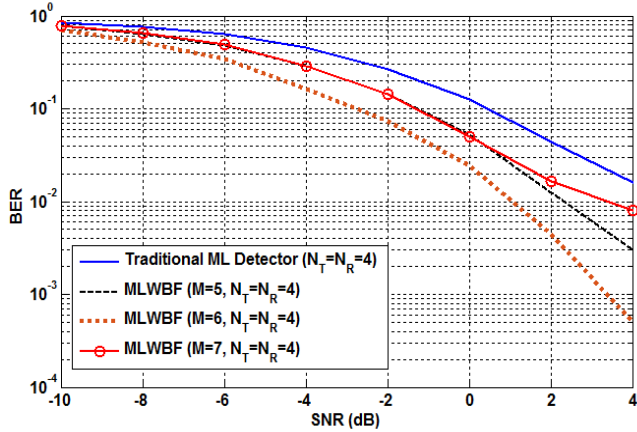


**Figure 9:** The BER versus SNR for MLWBF compared to the traditional ML detector for 4×4 LTE MIMO

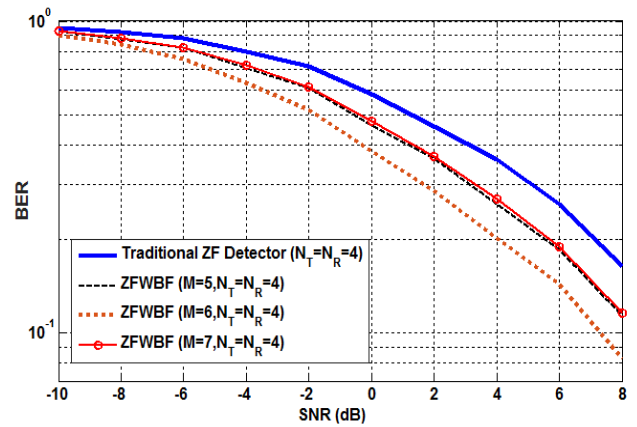


**Figure 10:** The BER versus SNR for ZF detector with beamforming (ZFWBF) compared to the traditional ZF detector for 4×4 LTE MIMO

**6.6. Test case 3: ZF Detector using Beamforming for 8 × 8 LTE MIMO System**

Replacing the 8-elements ULA by the 8-elements synthesized antenna arrays, it is found that the BER performance is significantly enhanced as the number of elements increase from  $M = 9$  to  $M = 14$  as shown in Figure 11. But, for  $M = 15$  and  $M = 16$ , the appearance of grating lobes highly degrades the BER performance as shown in Figure 12. The simulation results revealed that ( $M = 14, N_T = 8$ ) system provides the best BER

performance. For example, at  $SNR = 0\text{ dB}$ , the estimated BER is reduced from  $7.4 \times 10^{-1}$  for conventional ZF to  $4.5 \times 10^{-1}$  for ZFWBF using  $M = 14$  elements.

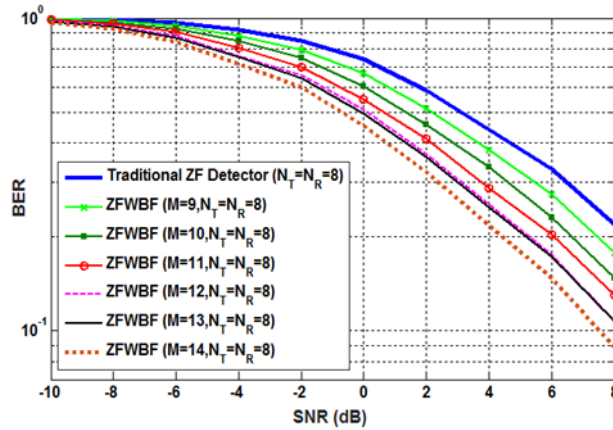


**Figure 11:** The BER versus SNR for ZFWBF using  $M=9,10,11,12,13,$  and  $14$  elements compared to the traditional ZF detector for  $8 \times 8$  LTE MIMO

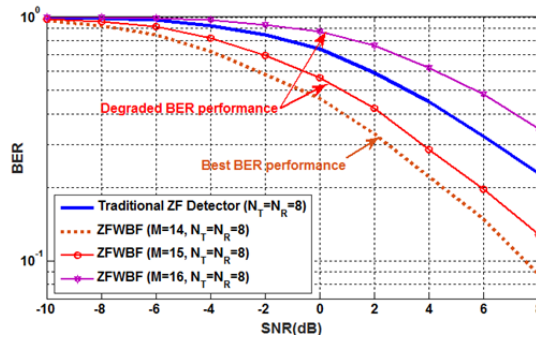


**Figure 12:** The BER performance degradation of ZF detector at  $(M \geq 15, N_T=8)$  for a  $8 \times 8$  MIMO system

**6.7. Test case 4: ZF detector using beamforming for overloaded MIMO system**

In this case, the  $4 \times 12$  MIMO is taken as a simulation target where the beamforming scenario (3) has been utilized. The employment of antenna arrays beamforming at both transmitting and receiving sides significantly improves the BER performance as shown in Figure 13. The simulation results showed that ZFWBF detector provides much lower BER than the traditional ZF detector. At  $SNR = -4\text{ dB}$ , the ZFWBF detector provides the same  $BER = 3 \times 10^{-3}$  as the traditional ZF detector at  $SNR = 0\text{ dB}$ .

**6.8. Test case 5: ZFWBF detector compared to related work**

Considering the beamformed  $4 \times 12$  MIMO in test case 4, the performance of the proposed ZFWBF detector is compared to the wavelet de-noising filter based ZF detector introduced in [7] and the hybrid ZF and ML detector introduced in [8] as shown in Figure 14. It is clear that the proposed detector has superior performance than these detectors under the same conditions.

**6.9. Capacity measurement of the proposed MIMO system**

**Test case 1: Capacity of proposed 4 × 4 MIMO**

For beamformed 4 × 4 MIMO, the capacities using  $M = 5$  and 6 elements are calculated and plotted as shown in Figure 15. For example, at  $SNR = -10$  dB the capacity of the traditional 4 × 4 MIMO is 0.81 bps/Hz. While the capacities of the proposed system using  $M = 5$  and 6 elements are 1.94 bps/Hz and 2.88 bps/Hz, respectively. The corresponding percentage capacity enhancement ratios  $\tilde{\eta}$  are 140.37 % and 257.46 %.

**Test case 2: Capacity of proposed 8 × 8 MIMO**

For beamformed 8 × 8 MIMO, the capacities for  $M = 9, 10, 11, 12, 13$  and 14 elements compared to the traditional 8 × 8 LTE MIMO are calculated and plotted as shown in Figure 16. At  $SNR = -10$  dB the calculated capacities are 2.01 bps/Hz, 2.7 bps/Hz, 3.45 bps/Hz, 4.01 bps/Hz, 4.57 bps/Hz, and 4.86 bps/Hz for  $M = 9, 10, 11, 12, 13,$  and 14, respectively while the capacity of the traditional 8 × 8 MIMO is 1.34 bps/Hz. The corresponding percentage capacity enhancement ratios  $\tilde{\eta}$  are 49.4 %, 101.27 %, 157.23 %, 198.8 %, 240.6 %, and 261.99 % respectively.

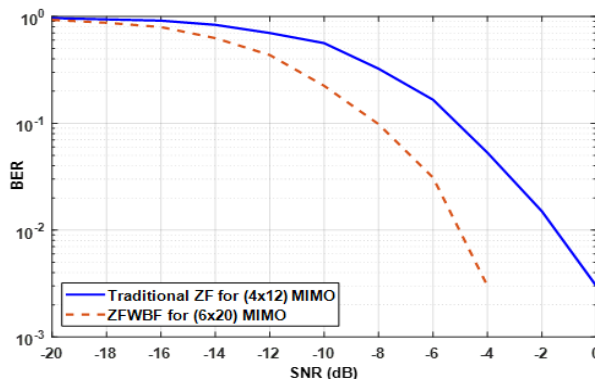


**Figure 13:** The BER versus SNR of the proposed ZFWBF detector using  $M_T=6$  and  $M_R=20$  elements compared to the traditional ZF detector

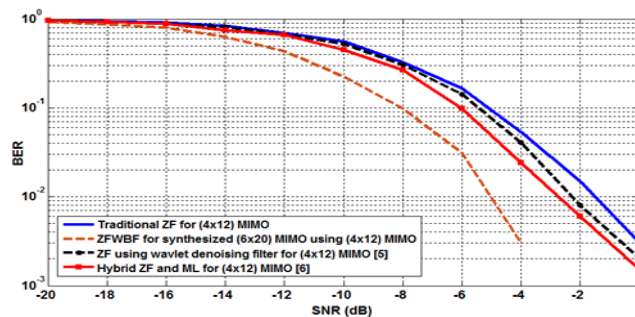


**Figure 14:** The BER versus SNR of the proposed ZFWBF detector using  $M_T = 6$  and  $M_R = 20$  elements compared to the 4 × 12 traditional ZF detector, the wavelet de-noising filter based ZF detector, and the hybrid ZF/ML detector

**Test case 3: Capacity of proposed  $4 \times 12$  MIMO**

Figure 17. Shows the system capacity versus SNR for beamformed  $4 \times 12$  MIMO system compared to the traditional  $4 \times 12$  MIMO. At  $SNR = -10$  dB the capacity is highly increased from 1.68 bps/Hz to 62.78 bps/Hz for the traditional and beamformed MIMO systems, respectively.

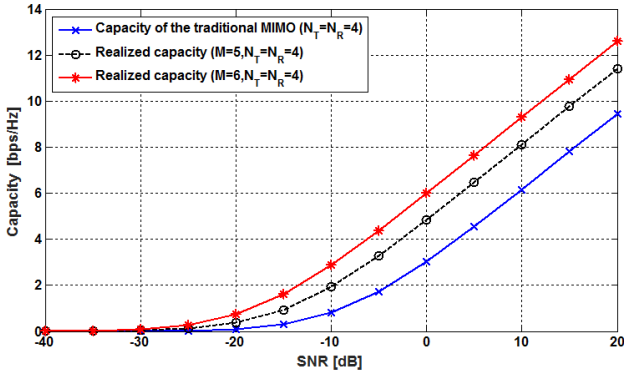


**Figure 15:** The system capacity versus SNR for the proposed  $4 \times 4$  MIMO system using  $M=5$  and  $6$  elements compared to the traditional  $4 \times 4$  LTE MIMO

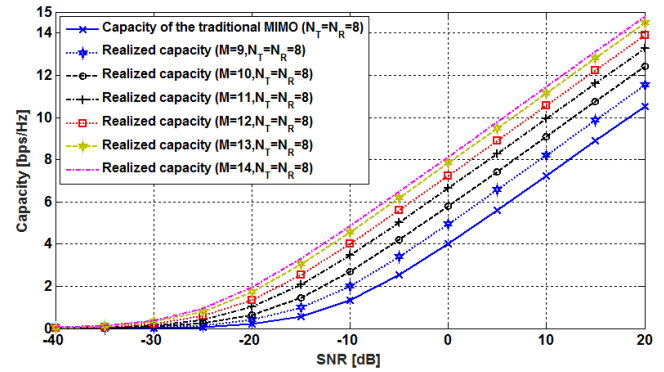


**Figure 16:** The system capacity versus SNR for  $8 \times 8$  MIMO system using  $M=9, 10, 11, 12, 13$  and  $14$  elements compared to the traditional  $8 \times 8$  LTE MIMO

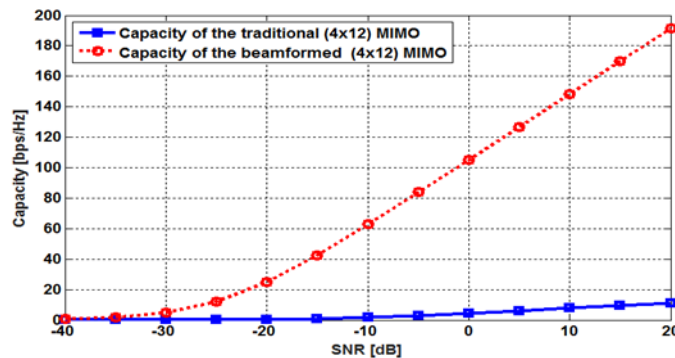


**Figure 17:** The system capacity versus SNR for beamformed  $4 \times 12$  MIMO system compared to the traditional  $4 \times 12$  MIMO

**7. Conclusion**

In this paper, a digital beamforming-based MIMO system was introduced for BER performance and capacity/spectral efficiency enhancement. The beamforming adjusts the elements excitations and spacing to synthesize higher gain antenna arrays without using additional antenna elements. The achieved arrays gain significantly increased the signal to noise ratio of the received signal. As a result, the BER is significantly reduced. The proposed MIMO signal model has been derived in a simple form which can be easily applied for state-of-the-art detection techniques. The simulation results proved that the beamforming-based detection techniques have superior performance in terms of BER and capacity/spectral efficiency than the traditional

techniques, wavelet denoising filter based detection techniques, and hybrid detection techniques.

## References

- [1]. Javornik, T., Kandus, G., Plevel, S., & Tomazic, S. (2008). MIMO: Wireless Communications.
- [2]. Sridhanya, A., Abhiram, Y., Guru, P. D., & Varsha, S. S. (2012). On the Design of MIMO-OFDM Transceivers via Geometric Mean Decomposition. *International Journal of Computer Applications*, 43(19), 7-14.
- [3]. Ali, A. B., Yung-Wey, C., Sabri, M. H., & Tat-Chee, W. (2015). On the Optimizing of LTE System Performance for SISO and MIMO Modes. *Third International Conference on Artificial Intelligence, Modelling and Simulation*, 412-416.
- [4]. Nidhi, K.M., & Suresh, R. H. (2016). Analysis of MIMO-OFDM using Different Modulation Techniques *International Journal of Computer Applications*. , 153(6), 37-40.
- [5]. J. Garcia-Frias and J. D. Villasenor, "Joint Turbo Decoding and Estimation of Hidden Markov Sources," in *IEEE Journal on Selected Areas in Communications*, vol. 19, no. 9, pp. 1671-1679, Sept. 2001.
- [6]. Ilmiawan, S., & Yukitoshi, S. (2017). Joint Turbo Decoding for Overloaded MIMO-OFDM Systems. *IEEE TRANSACTIONS ON VEHICULAR TECHNOLOGY*, 66(1), 433-442.
- [7]. Reham, W., Abd-Elsalam, Amr ,H. H., & Mahmoud ,A. A. (2016). Performance Enhancement of MIMO Detectors using Wavelet De-noising Filters. *International Journal of Engineering & Technology*, 5(4), 131-134.
- [8]. Samar, I. F., Mustafa, M. A. E., Amr, H. H., & Fathi E. A. (2016). Hybrid Techniques for Fast and Low Complexity MIMO Detection. *ICCTA 2016, 25-27 October 2016, Alexandria, Egypt*, 98-107.
- [9]. Vijay, V., & Alle-Jan, v. d. V. (2010). Analog Beamforming in MIMO Communications with Phase Shift Networks and Online Channel Estimation. *IEEE Transactions on Signal Processing*, 58(8), 4131–4143.
- [10]. Fouad, G., Javir, V., & Ignacio, S. (2011). Beamforming Design for Simplified Analog Antenna Combining Architectures. *IEEE Transactions on Vehicular Technology*, 60(5), 2373–2378.
- [11]. Le, L., Wie, X., & Xiaodai, D. (2014). Low-complexity Hybrid Precoding in Massive Multiuser MIMO Systems. *IEEE Wireless Communications Letters*, 3(6), 653–656.
- [12]. Shuangfeng, H., Chih-Lin, I., Zhikun, X., & Corbett, R. (2015). Large-scale Antenna Systems with Hybrid Analog and Digital Beamforming for Millimeter Wave 5G. *IEEE Communications Magazine*, 53(1), 186–194.
- [13]. Liu, Y., Nie, Z., & Liu, Q. H. (2008). Reducing the Number of Elements in a Linear Antenna Array by the Matrix Pencil Method. *IEEE Trans. Antennas Propag.*, 56(9), 2955-2962.
- [14]. Liu, Y., Liu, Q. H., & Nie ,Z. (2010). Reducing the Number of Elements in the Synthesis of Shaped-beam Patterns by the Forward-backward Matrix Pencil Method. *IEEE Trans. Antennas Propag.*, 58(2), 604-608.
- [15]. Liu, Y., Nie, Z., & Liu ,Q. H. (2010). A New Method for the Synthesis of Non-uniform Linear Arrays with Shaped Power Patterns. *Progress In Electromagnetics Research*, 107, 349-363.
- [16]. Kumar, B. P., & Branner , G. R. (1999). Design of Unequally Spaced Arrays for Performance

- Improvement., IEEE Trans. Antennas Propag., 47 (3) , 511–523.
- [17]. Marcano, D., & Duran , F. (2000). Synthesis of Antenna Arrays using Genetic Algorithms. IEEE Antennas Propag. Magazine, 42(3), 12-20.
- [18]. Kurup, D. G., Himdi, M., & Rydberg, A. (2003). Synthesis of Uniform Amplitude Unequally Spaced Antenna Array using the Differential Evolution Algorithm. IEEE Trans. Antennas Propag., 51(9), 2210–2217.
- [19]. Amr, H. H., Haythem, H. A., Ahmed , M.S., Salah, K., & Mohamed, N. (2011). Optimum Design of Linear Antenna Arrays Using a Hybrid MoM/GA Algorithm. IEEE, Antennas and Wireless Propagation Letters, 10,1232-1235.
- [20]. Ho, S. L., & Shiyou , Y. (2009). Multiobjective Synthesis of Antenna Arrays using a Vector Tabu Search Algorithm. IEEE Antennas Wireless Propag. Lett., 8, 947-950.
- [21]. Murino, V., Trucco, A., & Regazzoni, C. S. (1996). Synthesis of Unequally Spaced Arrays by Simulated Annealing. IEEE Trans. Signal Process., 44(1), 119–122.
- [22]. Kesong, C., Xiaohua , Y., Zi , S., H., & Chunlin Han (2007). Synthesis of Sparse Planar Arrays using Modified Real Genetic Algorithm. IEEE Trans. Antennas Propag. , 55(4), 1067–1073.
- [23]. Jin , N., & Rahmat-Samii , Y. (2007). Advances in Particle Swarm Optimization for Antenna Designs: Real-number, Binary, Single-objective and Multi objective Implementations. IEEE Trans. Antennas Propag., 55(3) , 556–567.
- [24]. Yong, S. C., Jaekwon , K., Won, Y.Y., & Chung-Gu, K. (2010). MIMO-OFDM Wireless Communications With MATLAB. Singapore: Wiley.
- [25]. Constantine, A. B. (2005). Antenna Theory: Analysis and Design, 3rd ed., New York, Wiley.